Deep Neural Network Feasibility Using Analog Spiking Neurons

Thomas Soupizet, Zalfa Jouni, Joao Frischenbruder Sulzbach, A. Benlarbi-Delai, Pietro Maris Ferreira

AUTHOR VERSION

Deep Neural Network Feasibility Using Analog Spiking Neurons

Thomas Soupizet, Zalfa Jouni, Joao Frischenbruder Sulzbach, Aziz Benlarbi-Delai, Pietro M. Ferreira,

Université Paris-Saclay, CentraleSupélec, CNRS, Lab. de Génie Électrique et Électronique de Paris, 91192, Gif-sur-Yvette, France.

Sorbonne Université, CNRS, Lab. de Génie Électrique et Électronique de Paris, 75252, Paris, France.

Email: tsoupizet@gmail.com, maris@ieee.org

Abstract—Novel non-Von-Neumann solutions have raised based on artificial intelligence (AI) such as the neuromorphic spiking processors in either analog or digital domain. This paper proposes to study the deep neural network feasibility using ultra-low-power eNeuron. The trade-offs in terms of deep learning capabilities and energy efficiency are highlighted. A linear fit model is found in the region of high energy efficiency of neuromorphic components. Thus, deep learning and energy efficiency mutually exclusive if those neuromorphic components are used.

Index Terms—neuromorphic circuits, spiking neural network, deep learning, low power

I. Introduction

The advent of industry 4.0 and the Internet of Things have pushed the requirements for smart processing capabilities in electronics. Along this advance, the smartness is also in a high energy efficient devices, which challenges common solutions. Since the 90's, neural networks and artificial intelligence solutions answered such need of high processing capability, and are thus widely implemented on classic computing [1]. Those implementations, however, tend to be power-hungry using Von-Neumann architectures and cloud computing. While reduced pace in Moore's law has further disclosed architecture limitations, demanded alternative solutions [2].

In this context, novel non-Von-Neumann solutions have raised based on artificial intelligence (AI). One of the most researched nowadays is the neuromorphic spiking processors in either analog or digital domain [3]. In contrast of Von-Neumann architecture, neuromorphic computing has appeared as an exciting alternative which provides edge computing capabilities for ultra-low-power applications [4]. Moreover, software and hardware solutions have brought the computational complexity of neural networks on energy efficient system with deep learning capabilities [5]. Both software and hardware solutions have pointed to the most widely used solution, which is the Feed-Forward Neural Networks (FNNs) [4]. Software implementations of FNNs are often used along with deep learning algorithms in order to solve highly complex problems. However, recent neuromorphic hardware is often single neuron circuits [6], [7], [8] or small neural networks [9], [10]. It is thus natural to ask if FNNs algorithms are usable on analog spiking neurons (eNeuron), to try and narrow the gap between hardware and software AI.

This paper objective is to study the deep neural network feasibility using ultra-low-power eNeuron. Previous published eNeurons from [9], [10] have been redesigned using in-house BiCMOS 55 nm technology from ST Microelectronics. Literature synapses are revised to propose a simple, linear, and weight reconfigurable one. Figure 1 illustrates the eNeuron and synapse model build up in this work from post-layout simulations. Further study of mathematical FNNs reveals set necessary conditions for deep learning using spiking neural networks. To the best of the author's knowledge, the trade-offs highlighted in terms of deep learning capabilities and energy efficiency are first proposed in this paper.

This paper is organized as follows. Section II revises literature in both hardware and software point of view. Finally, conclusions are drawn towards deep learning neural networks using ultra-low-power eNeurons.
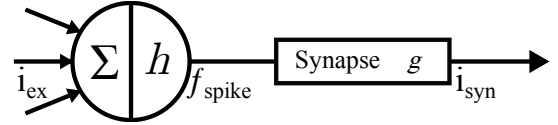

Fig. 1: Model spiking eNeuron and synapse. A neuron convert a current inputs to a spiking frequency. Synapse convert a spiking input to an output current.

II. Analog Spiking Neural Networks

Neuromorphic hardware aims to faithfully mimic biological systems in artificial neurons and synapses, illustrated in Fig. 1. Those devices have presented the best energy consumption per unit of information (i.e.E_{eff} in J/spike) and a competitive area trade-off. In the other hand, FNNs have been dominant in software AI research aiming deep learning capabilities and interested in mathematical network properties. Following subsections revise both hardware and software point of view.

A. Neurons

To design a neural network, one should first select a mathematical model for the neurons. The eNeuron model sets the degrees of complexity and biological accuracy as explained in [4]. Many popular models have seen widespread use as they offer different trade-offs among energy efficiency and computational capabilities. The simplicity of McCulloch-Pitts

(a) LIF model proposed in [8]

(b) ML model proposed in [7]
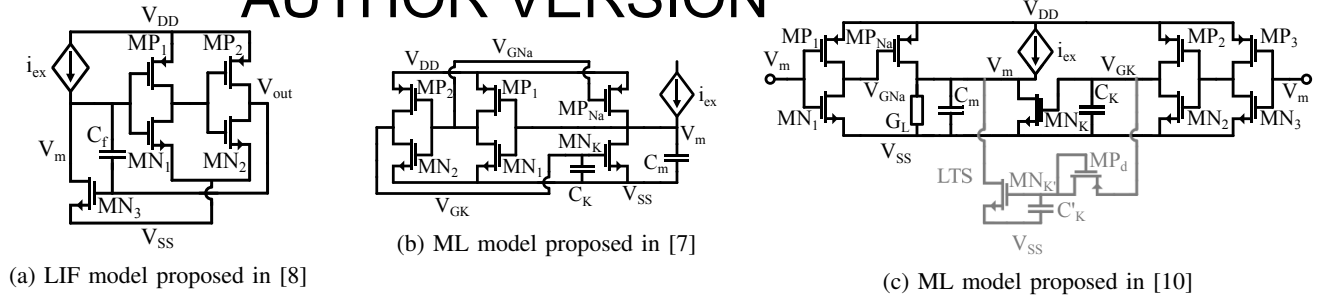
(c) ML model proposed in [10]

Fig. 2: eNeuron circuits studied. By using low supply-voltages, low membrane capacitance, and subthreshold transistors, authors have minimised power-consumption and surface area.

eNeurons makes them dominant in software implementations, as they only use an activation function to associate an output to the sum of their inputs.

More biologically inspired models mimic the spiking behavior of biological neurons. Among them, the (Leaky) Integrate-and-Fire (LIF), and Morris Lecar (ML) models stand out due to their widespread adoption in the literature. LIF eNeuron offers a spiking behavior at a low complexity by modeling the charge of a neuron. Figure 2(a) illustrates a LIF eNeuron proposed by Danneville et al., which is an Axon-Hillock topology. By using parasitic capacitors as the membrane capacitance (C_m), Danneville's eNeuron achieved both low energy consumption and low surface area, which could lead to the design being used in SNNs [8]. The LIF eNeuron has a mathematical model described in the literature as

$$V_m = \frac{1}{C_m} \int i_{ex} \left(e^{\frac{V_{DD} - V_m}{\eta \phi_t}} - e^{\frac{-2V_m}{\eta \phi_t}} \right) dt, \qquad (1)$$

where V_m is the spiking voltage signal; i_{ex} is the input excitation current; V_{DD} is the eNeuron supply voltage; η is the subthreshold slope; ϕ_t is the thermal voltage ($k_b T/q$). A detailed modeling is presented in [11].

The ML model provides behavior close to biological neurons by using multiple complex non-linear differential equations. Such eNeuron has recently been used to implement artificial neural networks, achieving tasks such as edge recognition [9] and audio signal processing [10]. Two common concerns in such edge computing applications are circuit surface and energy consumption. The popular figure of merit E_{eff} is used to assess the later. The E_{eff} is depicted considering the spike as a unit of information. State-of-the-art eNeurons [9], [10] are most efficient when they function at high spiking frequency, and they become increasingly E_{eff}-inefficient as spiking frequency lowers. ML eNeuron has a mathematical model described in the literature, being a non-linear function

$$V_m = -V_{DD} \cdot \tanh \left(\frac{G_L \cdot \sum i_{ex}}{\eta \phi_t} + \frac{1}{2} \ln \left(\frac{G_N}{G_P} \right) \right), \qquad (2)$$

where G_L is the equivalent conductance between eNeuron membrane and ground; G_N/G_P are the transistors' aspect ratio (NMOS conductance over PMOS conductance). A detailed modeling is presented in [7].

To address large-scale applications where energy dissipation is critical, Sourikopoulos et al. have proposed a simplified ML eNeuron illustrated in Fig. 2(b). By minimizing supply voltage and membrane capacitance, the authors achieved both low power consumption and high-spiking frequency to a high E_{eff} [7]. As a step towards SNNs, Ferreira et al. have implemented a Neuromorphic Analog Spiking-Modulator, which translated a sample input into a spiking output. The output layer is composed of two neurons with different spiking behavior, named 'LTS' and 'FS' eNeuron. Figure 2(c) illustrates both eNeuron, which are differentiated by the additional branch in blue, only present in the 'LTS' one. Recent ML eNeuron implementations notably make use of subthreshold transistors to reduce surface and power consumption [7], [10].

Literature results highlight the widely different performances in different areas and f_{spike}. For this reason, eNeurons depicted in Fig. 2 shall be implemented, in this work, with in-house tools. Thus, this work may propose a mathematical model from post-layout simulations. Moreover, the use of the same technology and simulator for eNeurons will prevent the result from being skewed by technology improvements, which will make the comparison between eNeuron models fairer.

B. Synapses

In spiking neural networks, neuron input (post-synaptic signals) and output (pre-synaptic signals) do not have the same dimensions. It is thus necessary to link neurons using synapses, which convert spiking information in i_{syn} post-synaptic signal.

Bartolozzi and Indiveri have proposed a synapse design adequate for VLSI implementation. By using transistors operating in subthreshold, the proposed differential pair integrator synapse response is

$$I_{syn}(t) = I_0 \cdot e^{\frac{V_{syn}(t) - V_{DD}}{\eta \phi_t}}, \qquad (3)$$

where I_0 is the leakage current; V_{syn} is the pre-synaptic signal ; I_{syn} is the post-synaptic signal. This model fits closer to the Destexhe mathematical model for synapses [12]. It is remarkable that the mean current output of the synapse is a linear function of the pre-synaptic f_{spike} [13].

In order to build an SNN, Danneville et al. have proposed two new synapses in [9]. The first proposition uses inverters along with a transimpedance amplifier and a transistor biasing

to generate the post-synaptic current. The second proposition implements an RC filter with two additional inverters. Those additional inverters extend the duration of the pre-synaptic pulse to produce a longer post-synaptic current pulse. The transimpedance is thus controlled by steep voltage pulses generated by the output of the inverters having an amplitude of $2 \cdot V_{DD}$.

Aforementioned synapses will serve as inspiration for this work. Figure 3 illustrates the synapses under study. Such synapse is composed of an RC filter, followed by a transimpedance, a current mirror, and a diode-connected transistor. Studied synapse shall attempt to balance advantages and drawbacks between Destexhe mathematical model agreement, ultra-low power, and plasticity. Plasticity is found in the current mirror architecture from [6], where current gain is a weighted bias signal. Ultra-low power is observed in the choice of passive RC filter from [9]. However, one can observe that eNeurons already have two inverters introduced in [9], which could be reused for further reduction in power consumption.
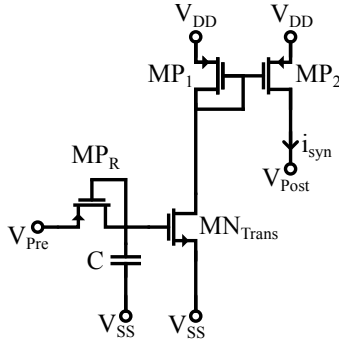

Fig. 3: Studied Synapse Circuit

C. Neural Networks

As early as 1989, it was demonstrated that a combination of a single non-linear function and affine functional can approximate an extensive range of functions [14]. This proved that FNNs with a nonlinear activation function and a hidden layer could solve a wide range of problems. Thus, the potential of deep-learning algorithms has been revealed, and more advanced neural networks have been implemented since then.

Because of their simplicity and performance, FNNs have been dominant in software AI research. They are structured in layers of neurons, which are only connected to neurons of the next layer. The input of a layer is therefore the output of the previous layer. This simplicity has led to more complex structures, which use different types of connections, such as convolution layers, or max-pooling layers [15].

By contrast, analog neural networks have focused on an optimal E_{eff} by an increasing f_{spike} [9], [10]. Observing (1) and (2), one may find that eNeuron models are sufficiently non-linear as required in software AI research literature. Concluding that deep-learning algorithms are an easy effort of implementation, without considering recent eNeurons, is at least unwise. Recent research focus has led to highly optimized

eNeurons and synapses, but a lower interest is presented in global network properties. When networks are built, the main figure of interest remains power consumption and the information is coded in a spiking occurrence [9]. Equations (1) and (2) are non-linear functions of voltage and current signal relationship, which does not assure a non-linear relation between f_{spike} and i_{ex} represented in Fig. 1. Besides, the usual design choice on transistor-based synapses modeled by (3) only reinforces the linear dependency of function and affine functionals.

III. DEEP NEURAL NETWORK FEASIBILITY ANALYSIS

While mathematical properties of analog neural networks are rarely a priority, E_{eff} of advanced software neural network architectures is rarely studied [4]. The tools used for software neural networks could be most useful in implementing deep learning for analog neural networks as [9]. Thus, it is important to bridge the gap between software AI, and analog neural network research subjects. To the best of the author's knowledge, the deep-learning feasibility in analog spiking FNNs has never been studied. Moreover, the trade-off between best E_{eff} and sufficient non-linearity has never been revealed. Answer those questions is the subject developed in this section.

A. Analysis of software neural networks

Literature has been interested by FNNs. Such networks have an input and an output layer, linked together by one or more hidden layers. An example network is depicted in Fig. 4(a), displaying a hidden layer N_{2k}. Neurons of a given layer only have the output of the previous layer as an input, hence the name Feed Forward. The output of a given layer is thus only dependent on the output of the previous layer.

A neuron model takes an input i and provides an output f. The relation between input and output can be described with an activation function h, which provides the relation $f = h(i)$. Given that in an FNN, neurons are organized in layers (see Fig. 4), one may describe the inputs and outputs of every neuron as vectors for the layer as

$$\begin{aligned} I &= (i_1, i_2, \ldots, i_n)^T \\ F &= (f_1, f_2, \ldots, f_n)^T \\ F &= (h_1(i_1), h_2(i_2), \ldots, h_n(i_n))^T \\ F &= H(I). \end{aligned} \tag{4}$$

Furthermore, as the input of the neurons are a linear combination of the output of the previous layer, we can define a matrix C_k such that, with F_k as the output of a given layer, $\forall k \in [1, n]$, $F_k = H_k(C_k \cdot F_{k-1})$. Let us assume that H_k is linear. It can thus be expressed as the matrix $H_k = diag(h_{k1}, h_{k2}, \ldots, h_{kM})$, with M the number of neurons in the layer. F_k can thus be expressed as a matrix product of F_{k-1}, where $F_k = H_k C_k \cdot F_{k-1}$. This leads by induction to the mathematical property of FNNs [5]

$$F_N = \prod_{k=1}^{N} H_k C_k \cdot I_0. \tag{5}$$

(a) An example software neural network.

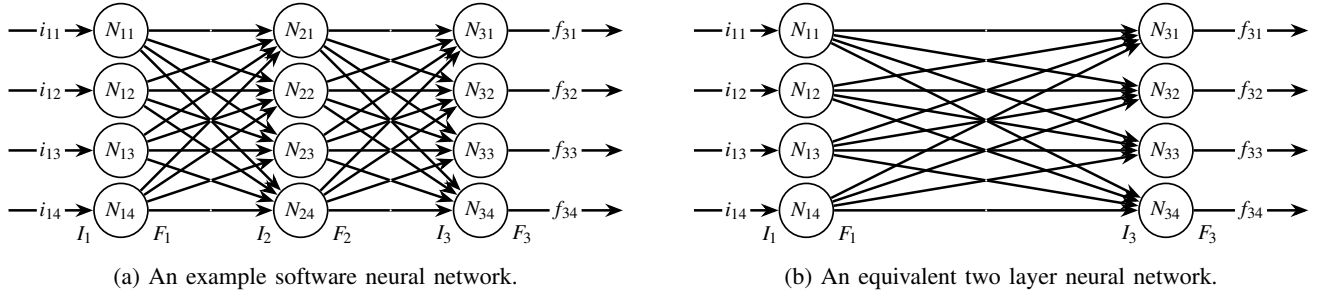(b) An equivalent two layer neural network.

Fig. 4: Feed-Forward Neural Networks. In the case of linear activation functions, a network with no hidden layer such as (b) can be found with the same transfer function as any (a).

The output F_N of the FNN is given by a linear combination of the input I_0. It is possible to find an equivalent two layers neural network, as represented in Fig. 4(b), where those two FNNs are equivalent. Having a linear activation functions, it thus hinders FNN to have the properties of a deep neural network, even with multiple hidden layers. For deep learning purposes, a non-linear activation function is needed. In literature, the non-linear functions *ReLU* and *tanh* are often used as activation functions. The latter is often related to eNeuron models (1) and (2).
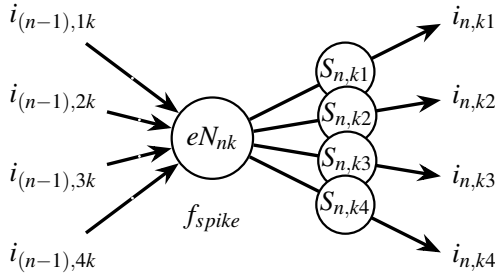

Fig. 5: Electronic Neural Network

B. Analysis of electronic spiking neural networks

While (5) and FNN property are widely known in the case of mathematical neural networks [14], it is not the case for electronic spiking neural networks (eNN). Figure 5 illustrates a system model for eNeurons (eN_{nk}) connected to a synapse array ($S_{n,ki}$). Considering eNNs, the presence of a synapse linking the neurons modifies the proof in (5). An eNeuron takes as an input current i_{ex}, which is the sum of the current fed ($\sum_{i=1}^{4} i_{(n-1),ik}$) in the node V_m. It outputs a spiking voltage in V_m which i_{ex} amplitude is coded in the f_{spike}. A function h can thus be defined for the eNeuron such that $f_{spike} = h(i_{ex})$. The synapse does the opposite, it converts f_{spike} pre-synaptic information to a post-synaptic current i_{syn}. From i_{syn} and f_{spike} relationship, a function g can be defined such that $i_{syn} = g(f_{spike})$.

An eNN such as the one modeled in Fig. 4(a), now considering eNeuron models from Fig. 5, can be studied with some formalisms. The kth eNeuron on the nth layer will be referred to as eN_{nk}, with the transfer function h_{nk}, input i_{nk}, and spiking frequency f_{nk}. The synapse linking together eN_{nk} and $eN_{(n+1)l}$ will be referred to as $S_{n,kl}$, with the transfer function $g_{n,kl}$, input $f_{n,kl}$, output $i_{n,kl}$. Let M_n be the number of neurons in layer n. Assuming the transfer functions of the synapses and neurons are linear, i.e. for all n,k,l such that $eN_{nk}, eN_{(n+1)l} \in eNN$:

$$h_{nk}(i_{ex}) = k_{nk} \cdot i_{ex} + b_{nk} \tag{6}$$
$$g_{n,kl}(f_{spike}) = w_{n,kl} \cdot f_{spike} + c_{n,kl}. \tag{7}$$

The spiking frequency of $eN_{(n+1)l}$ is then

$$f_{(n+1)l} = h_{(n+1)l} \left(\sum_{k=1}^{M_n} i_{n,kl} \right)$$

$$f_{(n+1)l} = h_{(n+1)l} \left(\sum_{k=1}^{M_n} g_{n,kl}(f_{nk}) \right)$$

$$f_{(n+1)l} = k_{(n+1)l} \cdot \left(\sum_{k=1}^{M_n} w_{n,kl} \cdot f_{nk} + c_{n,kl} \right) + b_{(n+1)l}. \tag{8}$$

This relation is linear, which means that if we express the spiking frequencies of a layer of eNeurons as a vector, we can find matrices such that

$$F_n = (f_{n1}, ..., f_{nM_n})^T \tag{9}$$
$$F_n = A_n F_{n-1}. \tag{10}$$

By induction, one may obtain

$$I_1 = (i_{11}, ..., i_{1H_n})^T$$

$$F_N = \prod_{n=1}^{N} A_n \cdot I_1. \tag{11}$$

This proves that the previous result still applies in the case of an eNN. Provided neurons and synapses have linear transfer functions, any multi-layer feed-forward neural network is equivalent to a two layers neural network.

IV. CIRCUIT DESIGN EXAMPLE

A i_{ex} parametric sweep is PLS simulated between 1 pA and 1 nA to extract the f_{spike} response of the eNeurons as a function of i_{ex}. At $i_{ex} > 1nA$, spiking frequency begins to fall due to circuit stability due to subthreshold biasing (i.e. spiking oscillations stops). Thus, the pointed i_{ex} range corresponds to the estimated dynamic of the eNeurons. This work will use the
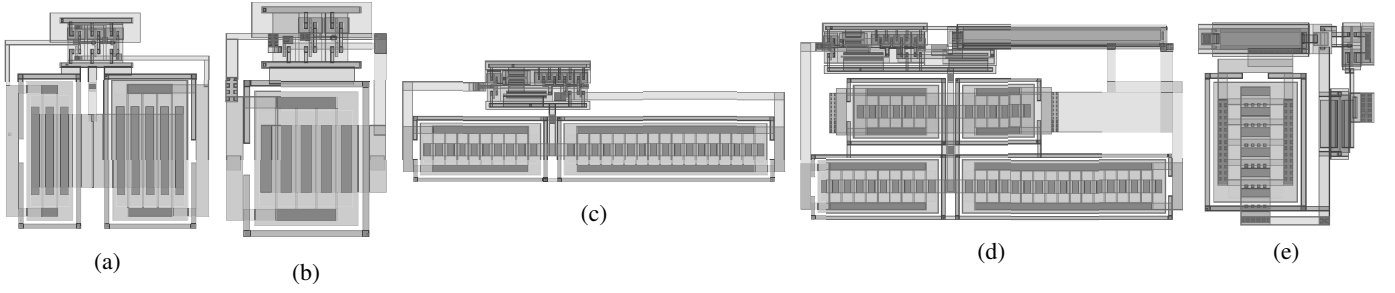
Fig. 6: In-house proposed layouts for eNeurons under test: (a) Simplified ML using $8.210 \times 7.525 \ \mu m^2$ [7], (b) LIF using $6.565 \times 4.335 \ \mu m^2$ [8], (c) "FS" biomimetic ML using $5.695 \times 17.335 \ \mu m^2$ [10], (d) "LTS" biomimetic ML using $9.110 \times 17.335 \ \mu m^2$ [10]. Studied synapse layout (e) using $6.60 \times 7.55 \ \mu m^2$.

least mean squares method to evaluate the transfer function linearity of aforementioned eNeurons. If an accurate linear fit is found for eNeurons under test, they should not be used in deep learning applications. Fitting accuracy is estimated from r^2 method from MatLab tools. Same PLS provide the relation between energy efficiency and spiking frequency, similarly tests are carried out as proposed in [9], [10].

TABLE I: Sizing of *MN* and *MP* transistors in $W \times L \ (nm)$ and in capacitance for C (fF) for the neurons

LIF model proposed in [8]		
$MP_1, MN_1, MP_2, MN_2, MN_3$		135×65
C_f	5.038	
ML model proposed in [7]		
$MP_1, MN_1, MP_2, MN_2, MP_{Na}, MN_K$		135×65
C_m	3.996	C_K	7.991
ML model proposed in [10]		
MP_1	135×60	MN_1	200×60
MP_2	1200×60	MN_2	135×60
MP_3	200×60	MN_3	135×60
MP_{Na}	800×60	MN_K	2000×60
C_m	5.534	C_f	9.838
MP_d	$500 \times 10,000$	$MN_{K'}$	2000×60
C_K'	6.763	G_L	Leakage
Proposed synapse		
MP_R	500×3000	MN_{Trans}	135×480
MP_1	270×60	MP_2	324×60
C	11.9		

In-house design is proposed for eNeurons illustrated in Fig. 2. eNeuron transistor sizing is summarized in Tab. I. Implementing every neuron in BiCMOS 55 nm technology, eNeuron layouts are depicted in Fig. 6. Post-layout simulations (PLS) are carried out using Spectre Virtuoso from BSIM4 models, which are measured-based foundry models validated in[16].

A basic synapse, illustrated in Fig. 3, was designed to assess the linearity characteristic of the Destexhe mathematical model in (3). A diode-connected transistor is used to have a high load, which makes the RC filter operate at a frequency in the range of spiking frequencies. The current mirror allows for choosing a weight for the synapse, and makes the output current positive. The last diode connected transistor allows for controlling the common-mode offset. Transistor and capacitor sizing are obtained so that the input and output ranges of the synapse match those of eNeurons. Table I summarizes the final sizing. Figure 6(e) illustrates the layout for the synapse under study. For PLS results, the synapse is used to connect two neurons, thus assuring the correct operation of the synapse.

A. eNeuron PLS

Figure 7 shows that the relations between i_{ex} and F_{spike} are non-linear, with energy efficiency significantly increasing with increased input current. As energy efficient is an important concern when designing and using eNeurons, it is expected for the neurons to be used in operating areas of high energy efficiency. Thus, a linear fit was realized for those areas in particular, omitting the less efficient low-spiking frequencies. Having a smaller range of operation, the LIF eNeuron proposed in [7] is significantly more non-linear than the other eNeurons. No satisfying linear fit could be found for the transfer function in Fig. 7(a), for any significantly large i_{ex} range.

For the eNeuron proposed in [8] and the FS eNeuron proposed in [10], a satisfying linear fit was found ($r^2 = 0.99$) for $i_{ex} > 200pA$. While the transfer functions are still non-linear in this area, they can be closely approximated by a linear function. The difference between the linear fits and real transfer functions on average of 1.58% of spiking frequency for Fig. 7(b), with the fit $f(i) = 0.10 \times i + 158.5$, and 3.09% for the FS eNeuron in Fig. 7(c), with the fit $f(i) = 0.28 \times i - 14.0$. For the LTS eNeuron proposed in [10], a linear fit can be found for the whole area of operation, with $r^2 = 0.99$) for $i_{ex} > 100pA$ with the fit $f(i) = 0.30 \times i + 133.9$.

Figure 7 also shows the energy efficiency of the neurons for a sweep of their input range. Figure 7(b) shows that the neuron becomes most energy efficient above $100pA$, with energy efficiency strongly degrading for small i_{ex}. Figure 7(c) show that the neurons become energy efficient at $i_{ex} > 200pA$, with performance degrading for smaller input. The neurons are thus expected to be used in ranges above $100pA$ and $200pA$ respectively.

This results highlights a trade-off that has to be made between energy efficiency and deep-learning capabilities while using state-of-the-art eNeurons. If a designer chooses to use the full range of frequency of the eNeurons, he will face poor energy efficiency. If instead one chooses to limit the

(a) eNeuron proposed in [7]   (b) ULP eNeuron proposed in [8]   (c) eNeurons proposed in [10]
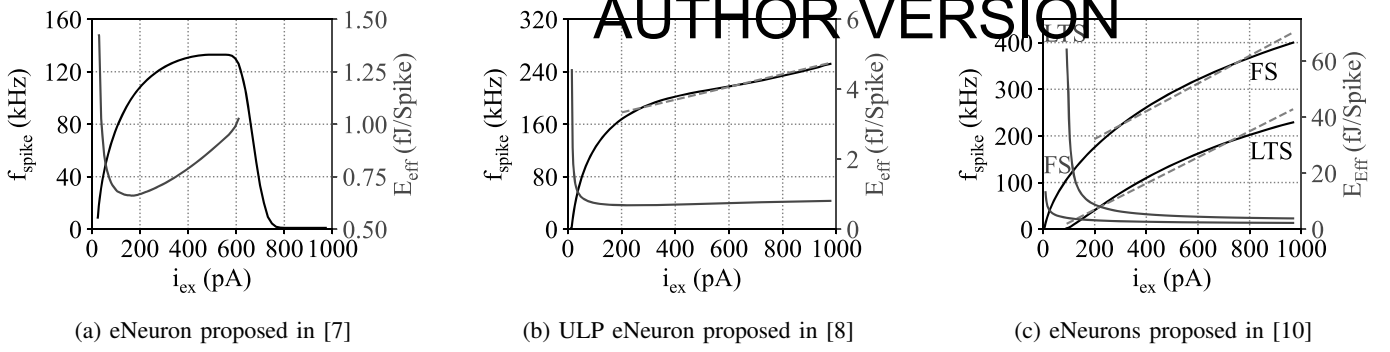
Fig. 7: Results of in-house PLS using BiCMOS 55nm technology. In black, spiking frequencies of eNeurons as a function of input current. In red, linearisation at high F_{Spike}. In blue, energy efficiency of the neurons as a function of the input current.

operating range to higher f_{spike}, the neurons will have a linear characteristic. In this second case, he will either be limited to the processing capabilities of a shallow neural network, or have to use a non-linear synapse. A designer could also use the Sorikopoulos eNeurons, which would provide nonlinearity at the cost of dynamic range.

B. Synapse PLS

The synapse PLS results exhibit the necessary functions: output current grows with input spiking frequency, and frequency injection is prevented. The excitation current of the input neuron was swept from 0 to 1 nA, to generate a sweep of the input spiking frequency of the synapse.
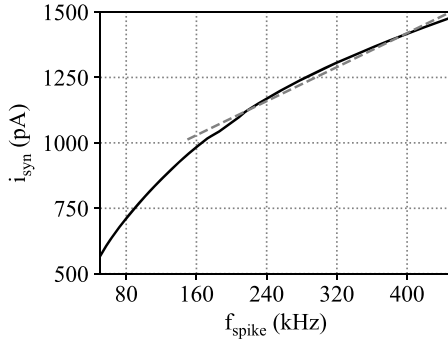

Fig. 8: Synapse transfer function in black, with linear fit in red.

Figure 8 shows that the output current of the synapse increases with the input frequency, which is consistent with the expected behavior for an excitation synapse. The frequency range explored is 0 to 450 kHz, as it is the output range of the FS Neuron used here [10]. The output is non-linear, however, as with the neurons, a linear fit can be found for a specific input range. For $f_{spike\,In} > 150\,kHz$, the linear fit $i(f) = 1.63 \times f + 769.2$ was found with $r^2 > 0.99$, with an average difference between linearization and output of 1.09%.

As a linear fit can be found for the synapse in areas of high energy efficiency, it will not introduce non-linearity for networks functioning in those areas of operation.

This means that the transfer function between the outputs of two layers will be a linear combination. This makes deep learning and energy efficiency mutually exclusive if those neuromorphic components are used.

V. CONCLUSIONS

This paper studied the deep learning capabilities of eNeurons, exposing trade-offs for using FNN architecture. PLS results showed that linear fits were possible at $i_{ex} > 200\,pA$, with $r^2 \geq 0.99$, which makes deep networks useless in those areas of high energy efficiency. A linear fit could also be found with $r^2 > 0.99$ for the synapse, showing that using such components at $i_{ex} > 200\,pA$ would not introduce any non-linearities. To the best of the author's knowledge, the trade-offs revealed in this paper are the first to highlight the counter-intuitive choice of high power consumption that has to be made to allow for deep learning capabilities.

REFERENCES

[1] D. Orrey, D. Myers, and J. Vincent, "A high performance digital processor for implementing large artificial neural networks," in *Proceedings of the IEEE Custom Integrated Circuits Conference*. Orlando, FL, USA: IEEE, jul 1991, pp. 16.3/1–16.3/4.

[2] *The Quantum Limit to Moore's Law*, vol. 96, no. 8, aug 2008.

[3] C. S. Thakur *et al.*, "Large-Scale Neuromorphic Spiking Array Processors: A Quest to Mimic the Brain," *Front. Neurosci.*, vol. 12, pp. 1–37, dec 2018.

[4] C. D. Schuman *et al.*, "A survey of neuromorphic computing and neural networks in hardware," 2017. [Online]. Available: https://arxiv.org/abs/1705.06963

[5] K. Guo, S. Han, S. Yao, Y. Wang, Y. Xie, and H. Yang, "Software-Hardware Codesign for Efficient Neural Network Acceleration," *IEEE Micro*, vol. 37, no. 2, pp. 18–25, mar 2017.

[6] G. Indiveri *et al.*, "Neuromorphic silicon neuron circuits," *Frontiers in Neuroscience*, vol. 5, 2011. [Online]. Available: https://doi.org/10.3389/fnins.2011.00073

[7] I. Sourikopoulos *et al.*, "A 4-fj/spike artificial neuron in 65 nm cmos technology," *Frontiers in Neuroscience*, vol. 11, 2017. [Online]. Available: https://doi.org/10.3389/fnins.2017.00123

[8] F. Danneville, C. Loyez, K. Carpentier, I. Sourikopoulos, E. Mercier, and A. Cappy, "A sub-35 pw axon-hillock artificial neuron circuit," *Solid-State Electronics*, vol. 153, pp. 88–92, 2019. [Online]. Available: https://doi.org/10.1016/j.sse.2019.01.002

[9] F. Danneville, K. Carpentier, I. Sourikopoulos, M. Paindavoine, and C. Loyez, "Sub-0.3V CMOS neuromorphic technology and its potential application," in *Int. Conf. Content-Based Multimed. Index.* Lille, France: IEEE, jun 2021, pp. 1–6.

[10] P. M. Ferreira, J. Nebhen, G. Klisnick, and A. Benlarbi-Delai, "Neuro-morphic analog spiking-modulator for audio signal processing," *Analog Integr. Circuits Signal Process.*, vol. 106, no. 1, pp. 261–276, jan 2021.

[11] M. Daliri, P. M. Ferreira, G. Klisnick, and A. Benlarbi-Delai, "A comparative study between E - neurons mathematical model and circuit model," *IET Circuits Devices Syst.*, vol. 15, pp. 175–192, feb 2021.

[12] A. Destexhe, Z. Mainen, and T. Sejnowski, "Kinetic models of synaptic transmission," *Methods in Neuronal Modelling, From Ions to Networks*, vol. 2, pp. 1–26, 01 1998.

[13] C. Bartolozzi and G. Indiveri, "Synaptic dynamics in analog vlsi," *Neural computation*, vol. 19, pp. 2581–603, 11 2007.

[14] G. Cybenko, "Approximation by superpositions of a sigmoidal function," *Mathematics of Control, Signals and Systems*, vol. 2, no. 4, pp. 303–314, Dec 1989. [Online]. Available: https://doi.org/10.1007/BF02551274

[15] A. Krizhevsky, I. Sutskever, and G. E. Hinton, "Imagenet classification with deep convolutional neural networks," in *Advances in Neural Information Processing Systems*, F. Pereira, C. Burges, L. Bottou, and K. Weinberger, Eds., vol. 25. Curran Associates, Inc., 2012. [Online]. Available: https://proceedings.neurips.cc/paper/2012/file/c399862d3b9d6b76c8436e924a68c45b-Paper.pdf

[16] P. Chevalier *et al.*, "A 55 nm triple gate oxide 9 metal layers SiGe BiCMOS technology featuring 320 GHz f_T / 370 GHz f_{MAX} HBT and high-Q millimeter-wave passives," in *Int. Electron Devices Meet. IEDM*, San Francisco, CA, USA, dec 2014, pp. 3.9.1–3.9.3. [Online]. Available: 10.1109/IEDM.2014.7046978